CONSTRUCTION OF DIFFICULT DRY DOCK IN YOKOHAMA, JAPAN

By Tsutomu Kumamoto,[1] Hitoshi Kameda,[2] Masaru Hoshiya,[3] Member, ASCE, and Kiyoshi Ishii[4]

ABSTRACT: Almost all coastal construction works in Japan today are carried out under variable and severe site conditions and tight budgetary constraints. Construction works are so unstable that civil engineers often meet many difficulties: (1) Soil, water, and climate conditions are not covered by present engineering rules; (2) no appropriate engineering methods for solving them exist theoretically; and (3) project circumstances, despite their simplicity, differ from past empirical data or similar works. There are two components in solving these problems. The first is to strengthen basic engineering through an advanced construction technology. The second, which is the focus of this paper, is to scientifically integrate management technology, together with Japanese quality control or TQC (total quality control), into the construction process, e.g., utilization of statistical methods in execution planning, and participation of all organization members in quality control and QC circle activities. The interaction of both approaches in construction is illustrated in this paper through an actual project for a dry dock built without using cofferdams.

INTRODUCTION

A dry dock having dimensions of 180 m in length, 30 m in width, and 13.5 m in depth has been built at Yokohama, Japan. The three main constructional features of the dock are:

1. Location on sea. Dry docks have generally been constructed by excavating into land adjacent to the sea. The lack of space, however, has made it necessary to locate this dry dock completely out in the sea (Kumamoto and Hoshiya 1987). Resource reuse and cost profitability have further led to the utilization of an existing gravity-type quay wall, made of discarded ship hulls, as the portside wall of the dry dock.
2. Construction without using cofferdams. Dry docks have likewise been generally built with cofferdams. In this case, no cofferdams could be used because construction had to be undertaken without disturbing shipping navigation around the port and normal operations at the quays around the site; and also within the shortest possible time period equivalent to two-thirds that of general construction methods. Direct on-sea and underwater works have resulted in cost savings of $7,500,000.
3. Use of JOILUC (Jointless Underwater Concrete). Because of the construction undertaken, it was necessary to build high-grade permanent concrete structures at the dock entrance (e.g., horizontal sill and pump room). The qualities

[1]General Mgr., Dept. of Civ. Engrg. Estimating, Shimizu Corp., 2-16-1, Kyobashi, Chuo-ku, Tokyo 104, Japan.
[2]Engr., Shimizu Corp., Escondido Village, Stanford, CA 94305.
[3]Prof., Dept. of Civ. Engrg., Musashi Inst. of Tech., Tokyo, Japan.
[4]Mgr., Oosaki Res. Lab., Shimizu Corp., Tokyo, Japan.

Note. Discussion open until November 1, 1990. To extend the closing date one month, a written request must be filed with the ASCE Manager of Journals. The manuscript for this paper was submitted for review and possible publication on May 24, 1988. This paper is part of the ***Journal of Construction Engineering and Management***, Vol. 116, No. 2, June, 1990. ©ASCE, ISSN 0733-9364/90/0002-0201/ $1.00 + $.15 per page. Paper No. 24709.

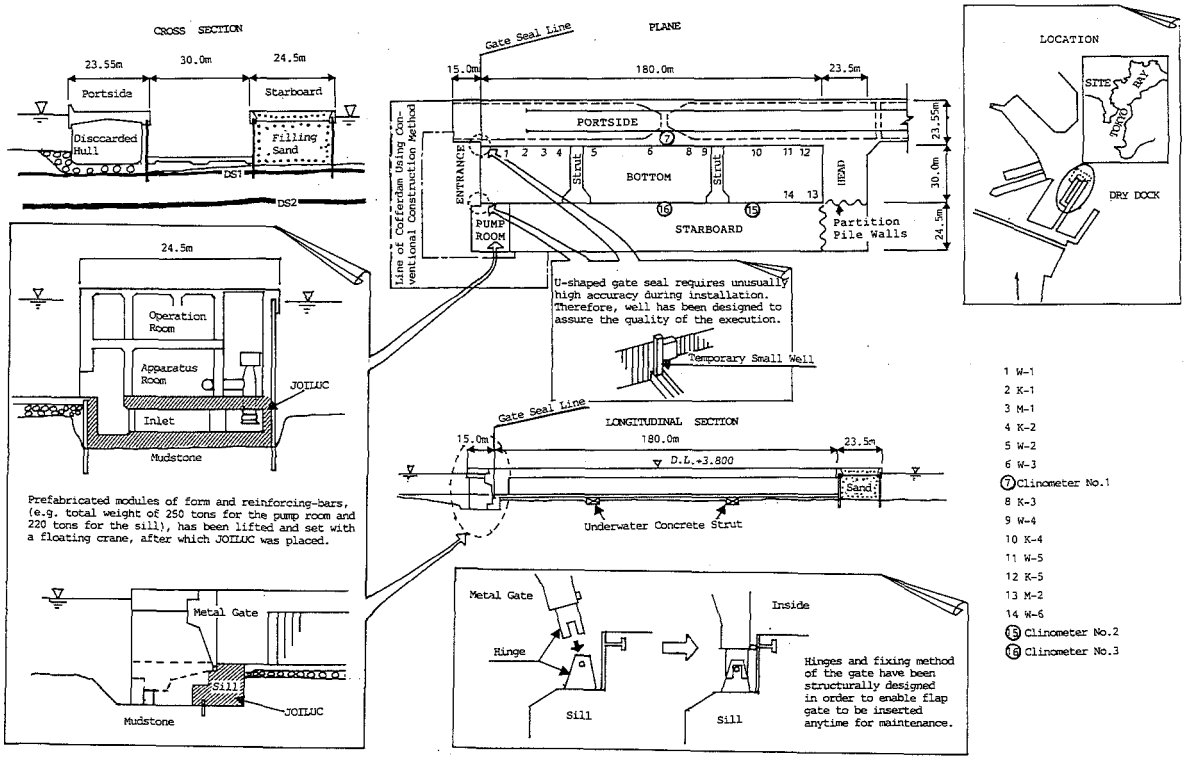

FIG. 1. Site Map and Plan of Dry Dock

J. Constr. Eng. Manage., 1990, 116(2): 201-220

required for marine concrete for such structures, in both its fresh and hardened states, are: workability, strength, durability, watertightness, and uniformity. Consequently, JOILUC (jointless underwater concrete) has been developed and was extensively used (3,000 m^3). JOILUC is a high-quality underwater concrete with superior flow properties that prevent segregation. It compensates for the shortcomings of conventional underwater concrete (e.g., prepacked concrete), and at the same time possesses all the desired qualities.

The site map and the dock's various innovations are shown in Fig. 1.

One special feature of dry dock structures is a watertight construction situated underwater from which water is either pumped in or out during normal operations within a very short period of 1–2 hours. Many issues arise regarding the underground water pressure exerted on the dock bottom, and engineers must take effective countermeasures against water pressure if problems are to be avoided in the future.

As a case study that demonstrates the construction management process (Peck 1969), this paper focuses on the instantaneous changes of relation between water pressure and the behavior of structures due to water level fluctuations as water is pumped both in and out of the dry dock. Due to the uniqueness and uncertainty of the dry dock, the management technology to this project differs significantly from those used in the manufacturing industry.

Description

Structure

The dry dock is structurally divided into five parts: the portside wall, the starboard and the head walls, the pump room, the entrance, and the dock bottom. All these parts seal off water.

The portside wall is constructed by driving sheet piles along the dock side of the existing quay wall to form a watertight curtain. The starboard and head walls are a watertight double pile wall structure composed of steel pipe piling on the inner side and steel sheet piling on the sea side. These piles are driven in parallel 24.5 m apart, and then connected to each other with tie-rods at the top. Finally, the open space between the inner and outer pile walls is filled using sand with an interfrictional angle of 35°.

The pump room is situated at the corner of the starboard wall and the entrance. It functions both to pump water in and out of the dock and as the vertical sill of the flap gate. It has been constructed using the newly developed JOILUC, as well as conventional concrete.

The U-shaped entrance structure is composed of vertical sills on the portside and starboard walls, and the horizontal sill. It has also been built using JOILUC. A flap gate with two hinges has been installed in the sill and serves to keep out seawater.

The dock bottom is a 70–90-cm-thick reinforced concrete slab foundation laid directly on the ground layer. Crushed gravel and perforated pipes placed underneath the slab act as a water pressure reducing system when water is pumped in and out during normal operations.

Execution

As indicated in Fig. 2, the total time alloted to the project from the commencement of work to the completion of all construction is sixteen months.

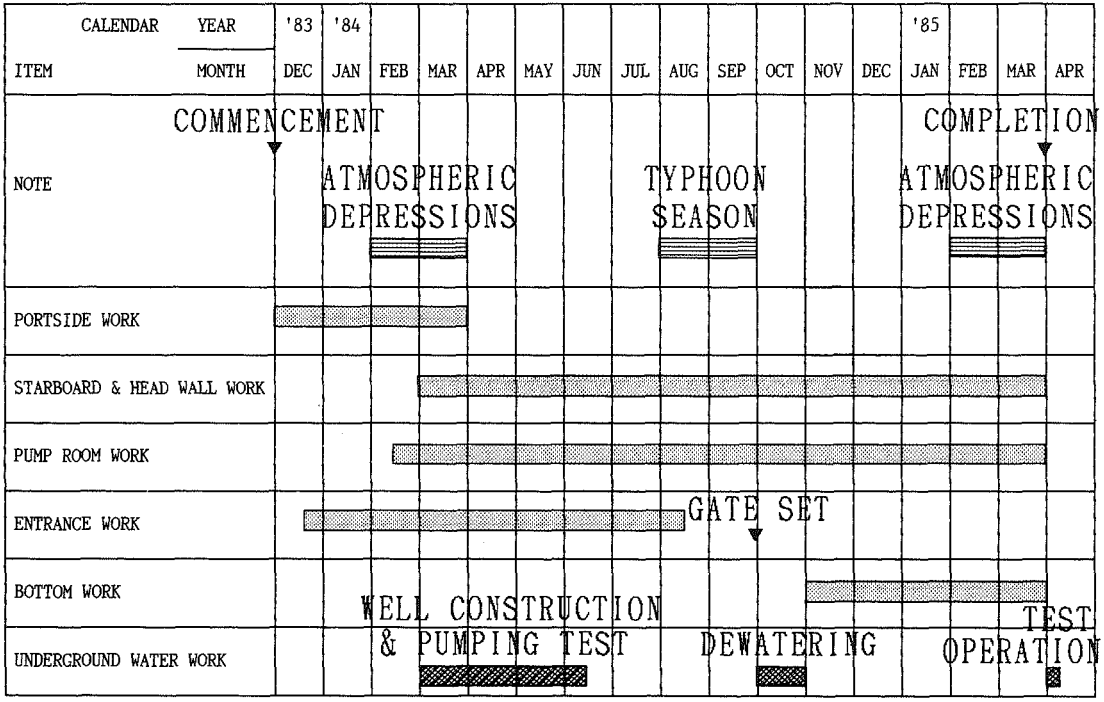

FIG. 2. Construction Schedule

J. Constr. Eng. Manage., 1990, 116(2): 201-220

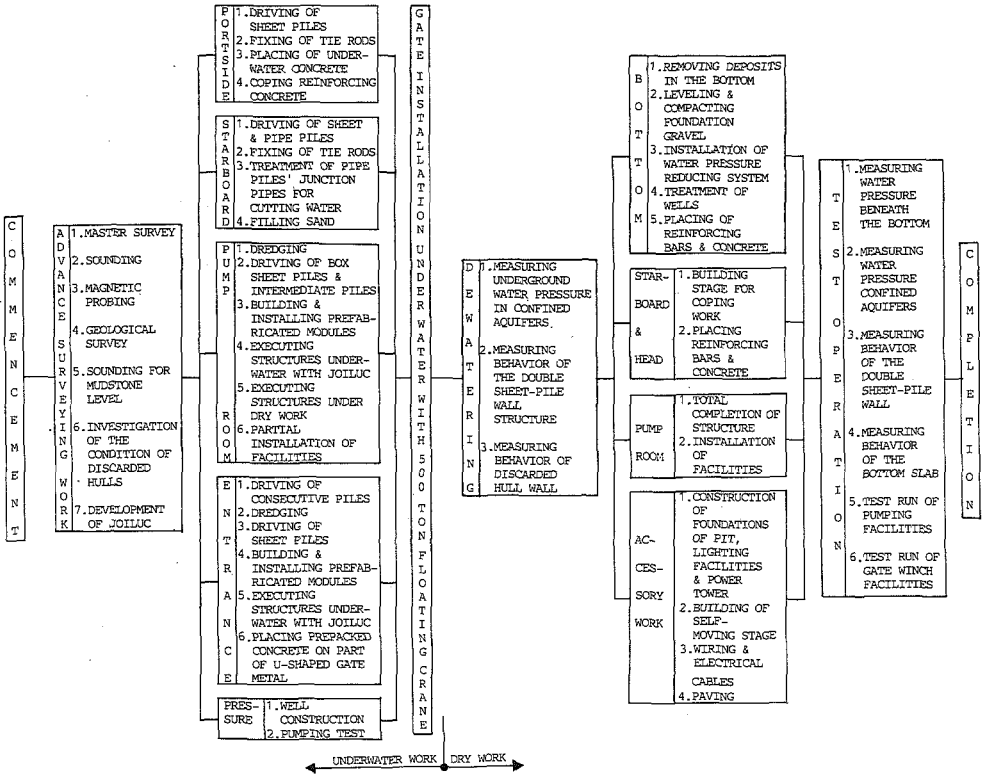

FIG. 3. Flowchart of Master Execution Plan

J. Constr. Eng. Manage., 1990, 116(2): 201-220

There were, however, three seasons of typhoons and atmospheric depressions within this period, each with dangers peculiar to on-sea construction. Ongoing works would be constantly exposed to severe conditions throughout the construction period, and on-site changes and deviations were expected to occur. It was necessary, therefore, to take into careful consideration all these variable factors and make a detailed execution plan. The master execution plan flow chart is shown in Fig. 3.

Underground Water Control

The structural features of the dry dock gave rise to two problems that had to be solved:

1. It was not possible to keep water out of the dock completely, because of its massive size and its location in the sea. Since the scale of pump facilities and the rate of running cost depend largely on the amount of water seepage, this volume had to be accurately understood so that adequate provisions could be made in the design of pump facilities and the type of water cut-off structures.
2. Should there be a confined aquifer, its head must fall low enough in relation to the gradually declining water level as water is pumped out of the dock so as to avoid the failure of the bottom slab. Underground water pressure must decline to a safe head within 1–2 hours.

Geological Profile

Tide level at the site is between D.L. ±0.00 (datum level) and D.L. +2.00 m. Sea bottom is D.L. −10.0 m. A 2-m-thick layer of deposits rests on the sea bottom, which is a solid mudstone layer with an N-value of at least 50. Confined aquifers exist in the solid mudstone. Relatively continuous sand layers lie approximately between D.L. −13 m and D.L. −14 m (DS1 layer) and D.L. −18 m (DS2 layer), and several sandwiched sand layers were found in isolated spots at approximately D.L. −15 m (sandwiched layers). The findings of the geological investigation are as follows:

1. The DS1 layer exists continuously.
2. The DS2 layer is continuous throughout the project site, but is intermittent considering the whole harbor.
3. The head of each confined aquifer is equal to the sea level or higher.
4. The thickness of the DS1 and DS2 layers are 15–35 cm and 10–20 cm, respectively. According to the JFT (Johnston formation tester) test, the permeability coefficients are $k = 1.00–1.07 \times 10^{-2}$ cm/s for DS1 and $k = 1.49–2.10 \times 10^{-3}$ cm/s for DS2.
5. Specific conductance tested in the boreholes is approximately 26,000–40,000 μs/cm, and is lower than that of sea water (50,000 μs/cm).

Measures against Underground Water

DS1 Layer

The steel sheet piles and steel pipe piles that encircle the dry dock were driven through the DS1 layer, so that seepage volume from the outside is considered to be minimal. In addition, underground water pressure is thought to be relieved as water is pumped in and out for several reasons.

First, the sea bottom around the site was once dredged 25 years ago almost to the depth of the DS1 layer in order to fix the discarded hulls for the quay wall. It was dredged again this time to the same depth for the purpose of building underwater concrete struts that would prevent the discarded hulls from sliding laterally before the bottom slab is constructed due to the difference of water pressure that would occur when the dock is dewatered.

Some boreholes driven before this project have been left unsealed, thus leaving a lot of passages through which underground water pressure is relieved naturally as the dock is dewatered. Observation wells were thus constructed to confirm the decline in head of the DS1 layer.

Layers Deeper than DS1

It was neither advantageous nor possible to cut off water seeping through confined aquifers deeper than the DS1 layer by sheet piling. Since these layers are relatively thin and their permeability coefficients are small, seepage was not considered to be serious. However, geological investigation reveals that each confined aquifer has a head equal to or higher than that of the highest tide level. Confined aquifers shallower than D.L. −30 m were therefore regarded as layers wherein pressure must be reduced to maintain the balance between the upward underground water pressure and the downward dead load pressure as the dock is dewatered.

Taking into account the whole work schedule, it was decided that construction would proceed while investigating and testing underground water pressure, and taking appropriate countermeasures. Wells of 200- and 100-mm diameters were constructed in accordance to the progress of other works and the investigation and testing of underground water pressure. These wells eventually function as relief wells.

Well Construction and Investigation and Analysis of Underground Water

Wells were constructed along the portside and the starboard walls, using these walls as support for the stagings (Fig. 1). As may be seen in Fig. 2, the wells made along the starboard wall would not be finished in time for them to be used for investigation since there is a time lag between the construction of the portside and starboard walls. Investigation into underground water has thus been limited to the wells along the portside wall. Four wells, W-1, W-3, W-5, and K-5, were constructed. Water was then pumped up from each well to determine if corresponding fluctuations in the other wells would occur. Findings revealed that except for W-5 and K-5, no correlated reactions took place in the other wells. Three hypotheses were thought to explain this phenomenon:

1. Seawater, not from the confined aquifer, was directly being pumped up due to an incomplete seal where the well meets the seabed.
2. Confined aquifers previously thought to be continuous are in actuality discontinuous.
3. Seawater leaks into the confined aquifers through open joints and cracks in the mudstone layer all throughout the dock bottom. This vertical leakage surpasses in volume the horizontal flow in the confined aquifers.

Many observations confirm the completeness of the wells' seals at the

TABLE 1. Results of Pump Test

Number (1)	Number (2)	m^3/min (3)	t (min) (4)	x (m) (5)	s (m) (6)	T (m^2/min)[a] (7)	S[a] (8)
			(a) Analysis No. 1				
K-4	W-5	0.0101	3,350 April 11 at 10:30 a.m. to April 13 at 6:20 p.m.	17.842	0.890	5.22×10^{-3} 4.82×10^{-3} 5.19×10^{-3} 3.25×10^{-3}	2.46×10^{-4} 4.44×10^{-4} 2.75×10^{-4} 3.93×10^{-4}
			(b) Analysis No. 2				
K-4	W-5	0.0116	4,010 April 21 at 9:20 p.m. to April 24 at 4:10 p.m.	17.842	0.990	6.68×10^{-3} 6.35×10^{-3} 6.21×10^{-3} 4.00×10^{-3}	4.53×10^{-4} 6.58×10^{-4} 5.11×10^{-4} 6.86×10^{-4}
			(c) Analysis No. 3				
W-5	K-4	0.0190	924 May 1 at 6:24 p.m. to May 2 at 9:49 a.m.	17.842	0.730	1.10×10^{-2} 1.35×10^{-2} 9.94×10^{-3} 6.43×10^{-3}	4.96×10^{-4} 4.37×10^{-4} 5.68×10^{-4} 1.09×10^{-3}
			(d) Analysis No. 4				
W-5	K-4	0.0500	1,068 May 8 at 2:37 p.m. to May 9 at 8:25 a.m.	17.842	2.480	8.17×10^{-3} 8.04×10^{-3} 7.26×10^{-3}	3.93×10^{-4} 4.81×10^{-4} 5.25×10^{-4}
			(e) Analysis No. 5				
K-1	W-1	0.0110	900 May 9 at 6:00 p.m. to May 10 at 9:00 a.m.	11.311	2.660	8.91×10^{-4} 6.74×10^{-4} 4.61×10^{-4} 5.00×10^{-4}	1.03×10^{-4} 1.58×10^{-4} 1.24×10^{-4} 1.30×10^{-4}
			(f) Analysis No. 6				
K-1	W-1	0.0063	3,780 May 22 at 7:00 p.m. to May 25 at 10:00 a.m.	11.311	2.466	1.11×10^{-3} 3.01×10^{-3} 1.01×10^{-3} 3.13×10^{-4}	2.54×10^{-4} 3.76×10^{-4} 2.97×10^{-4} 3.86×10^{-4}
			(g) Analysis No. 7				
K-4	W-5	0.0145	3,780 May 22 at 7:00 p.m. to May 25 at 10:00 a.m.	17.842	0.837	8.29×10^{-3} 5.42×10^{-3} 7.73×10^{-3} 5.33×10^{-3}	2.34×10^{-4} 3.20×10^{-4} 2.62×10^{-4} 3.17×10^{-4}
			(h) Analysis No. 8				
K-5	W-5	0.0145	3,780 May 22 at 7:00 p.m. to May 25 at 10:00 a.m.	4.327	1.783	2.65×10^{-3} 2.34×10^{-3} 1.93×10^{-3} 2.31×10^{-3}	1.47×10^{-3} 1.90×10^{-3} 1.85×10^{-3} 1.87×10^{-3}
			(i) Analysis No. 9				
K-3	W-4	0.0096	3,570 May 29 at 8:30 a.m. to May 31 at 8:00 p.m.	3.477	8.049	3.74×10^{-4} 3.03×10^{-4} 2.77×10^{-4} 3.02×10^{-4}	3.89×10^{-4} 5.56×10^{-4} 4.95×10^{-4} 5.45×10^{-4}

TABLE 1. (*Continued*)

(1)	(2)	(3)	(4)	(5)	(6)	(7)	(8)
			(*j*) Analysis No. 10				
W-3	W-2	0.0160	1,340 June 4 at 10:30 a.m. to June 5 at 8:50 a.m.	25.258	0.195	2.76×10^{-2} 1.77×10^{-2} 1.99×10^{-2} 1.65×10^{-2}	3.50×10^{-4} 8.80×10^{-4} 6.62×10^{-4} 8.61×10^{-4}
			(*k*) Analysis No. 11				
K-4	W-4	0.0152	1,140 June 5 at 1:30 p.m. to June 6 at 8:30 a.m.	27.187	0.347	1.34×10^{-2} 6.36×10^{-4} 9.87×10^{-3} 5.19×10^{-2}	8.59×10^{-5} 4.68×10^{-5} 1.08×10^{-4} 4.64×10^{-5}
			(*l*) Analysis No. 12				
W-5	W-4	0.0152	1,140 June 5 at 1:30 p.m. to June 6 at 8:30 a.m.	45.029	0.218	2.32×10^{-2} 2.02×10^{-2} 1.47×10^{-2} 1.79×10^{-2}	2.96×10^{-4} 3.42×10^{-4} 3.79×10^{-4} 3.21×10^{-4}
			(*m*) Analysis No. 13				
K-5	W-4	0.0152	1,140 June 5 at 1:30 p.m. to June 6 at 8:30 a.m.	49.356	0.140	3.48×10^{-2} 2.21×10^{-2} 2.55×10^{-2} 2.12×10^{-2}	1.67×10^{-4} 2.03×10^{-4} 2.08×10^{-4} 2.17×10^{-4}
			(*n*) Analysis No. 14				
K-1	W-2	0.0568	1,450 June 6 at 9:00 a.m. to June 7 at 9:00 a.m.	34.037	0.156	1.08×10^{-1} 3.38×10^{-2} 6.48×10^{-2} 3.41×10^{-2}	2.06×10^{-3} 3.11×10^{-3} 2.51×10^{-3} 3.10×10^{-3}
			(*o*) Analysis No. 15				
K-2	W-2	0.0568	1,380 June 6 at 9:00 a.m. to June 7 at 8:00 a.m.	18.865	0.282	4.16×10^{-2} 4.51×10^{-3} 1.39×10^{-2} 2.44×10^{-1}	7.63×10^{-4} 5.06×10^{-4} 7.54×10^{-4} 1.55×10^{-7}
			(*p*) Analysis No. 16				
W-3	W-2	0.0568	1,380 June 6 at 9:00 a.m. to June 7 at 8:00 a.m.	25.258	0.518	2.28×10^{-2} 1.13×10^{-2} 1.11×10^{-2} 1.10×10^{-2}	6.43×10^{-4} 9.77×10^{-4} 7.42×10^{-4} 9.77×10^{-4}
			(*q*) Analysis No. 17				
W-1	K-1	0.0054	1,000 June 8 at 4:20 p.m. to June 9 at 9:00 a.m.	11.311	1.730	9.28×10^{-4} 7.84×10^{-4} 6.95×10^{-4} 7.59×10^{-4}	1.26×10^{-4} 1.63×10^{-4} 1.56×10^{-4} 1.58×10^{-4}
			(*r*) Analysis No. 18				
W-5	K-5	0.0225	1,120 June 8 at 1:50 p.m. to June 9 at 8:30 a.m.	4.327	2.842	3.43×10^{-3} 2.73×10^{-3} 3.12×10^{-3} 2.69×10^{-3}	1.73×10^{-3} 2.33×10^{-3} 2.03×10^{-3} 2.35×10^{-3}

[a]The four values shown are for Jacob's solution, the Thesis equation curve, the Hantush-Jacob method, and the Hantush solution, respectively.

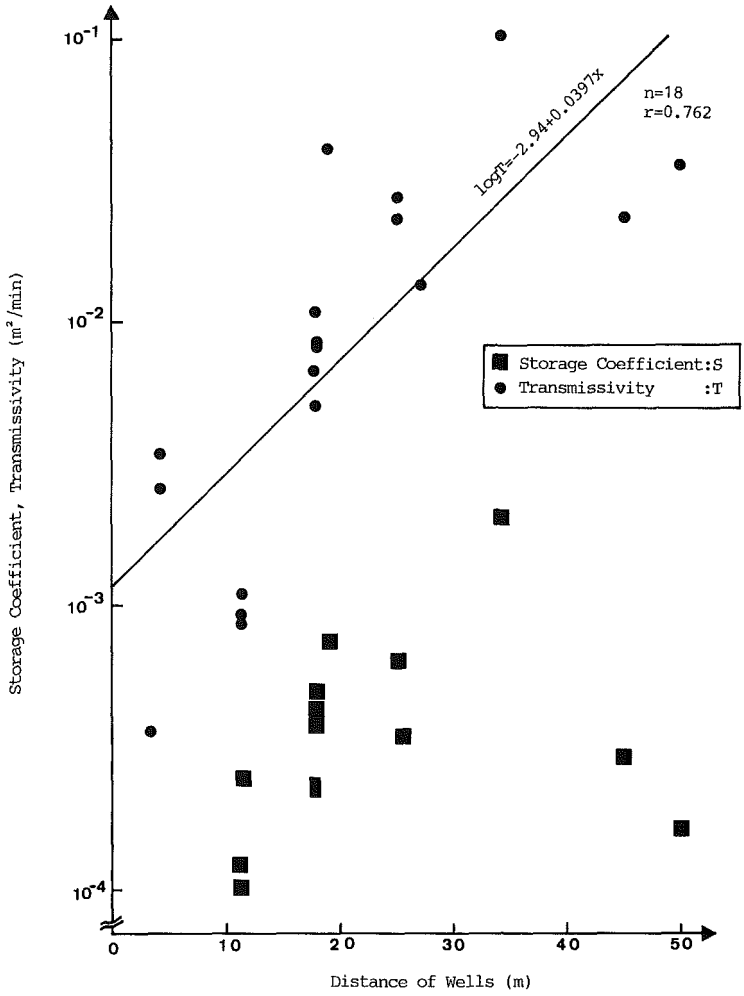

FIG. 4. Relation between Distance of Wells and Transmissivity Based on Jacob's Solution

seabed. First, the water level in the wells was higher than tide level by 10–20 cm, and there was likewise a lag between the periodic changes of water level in the wells and the sea, thus showing clearly that the fluctuations of the water level in the wells differed from that of tide level. Second, although the water level has been lowered and maintained at the bottom of the well, the pumping volume did not change with time. Third, the specific conductance of water obtained from the wells differed from that of the seawater.

Similarly, findings from both the boring tests and the construction of wells reveal the existence of sand at similar depths, thus confirming the continuity of at least the DS1 and DS2 layers.

The third hypothesis thus remains as the only possible explanation. More

TABLE 2. Relation between Distance of Wells and Transmissivity

Regression formula where T = transmissivity (m^2/min), x = distance (m) (1)	Correlation coefficient (correlation analysis) (2)	Analysis of Variance: Statistics (3)	Sum of square (4)	Degree of freedom (5)	Mean square (6)	Ratio of mean square (7)
(*a*) Analysis Based on Jacob's Solution						
$\log T = 2.94 + 0.0397x$	0.762 [$r(16,0.01) = 0.590$]	Regression	4.432	1	4.432	22.167[a]
		Residual	3.199	16	0.200	
		Total	7.631	17		
(*b*) Analysis Based on Thesis Equation-Type Curve Method						
$\log T = -2.98 + 0.315x$	0.680 [$r(16,0.01) = 0.590$]	Regression	2.779	1	2.779	13.757[a]
		Residual	3.234	16	0.202	
		Total	6.013	17		
(*c*) Analysis Based on Hantush-Jacob Method						
$\log T = -3.04 + 0.0376x$	0.756 [$r(16,0.01) = 0.590$]	Regression	3.977	1	3.977	21.339[a]
		Residual	2.982	16	0.186	
		Total	6.959	17		
(*d*) Analysis Based on Hantush Solution						
$\log T = -3.11 + 0.0398x$	0.640 [$r(15,0.01) = 0.606$]	Regression	4.449	1	4.449	10.395[a]
		Residual	6.427	15	0.428	
		Total	10.876	16		

[a]Highly significant.

wells were established and investigation was continued. Results of the investigation are summarized in Table 1. Results of the statistical analysis of data based on Jacob's solution in Table 1 are shown in Fig. 4 and Table 2, which also includes results obtained in the same manner using the Thesis equation-type curve method (Thesis 1935) and the Hantush-Jacob method (Hantush 1960).

The values of storage coefficient in Table 1 and Fig. 4 are nearly equal to the value of the confined aquifer, which is 1×10^{-3}–1×10^{-4}. However, an adequate correlation between transmissivity and the distance between pertinent wells, and an analysis of the variance table (Table 2) shows the regression equation to reflect the actual situation more clearly.

The increase of transmissivity in proportion to the distance between the wells simply indicates that vertical leakage from the sea through the open joints and cracks in mudstone layer surpassed greatly in volume the horizontal flow in the confined aquifers. These open joints and cracks function as natural relief wells for underground water pressure in the aquifers when the dock is dewatered.

DEWATERING FOR CONSTRUCTION

Rate of Dewatering

As indicated in the timetable, the dewatering phase immediately follows the installation of the gate. To achieve this, self-timing water-level registers were installed at each well in order to confirm the natural dissipation of underground water pressure in the aquifers through the open joints and cracks in the mudstone layer during dewatering.

Control limits for dewatering are defined by the depth of the shallowest confined aquifer each well aims at. It is thus possible to safely pump out

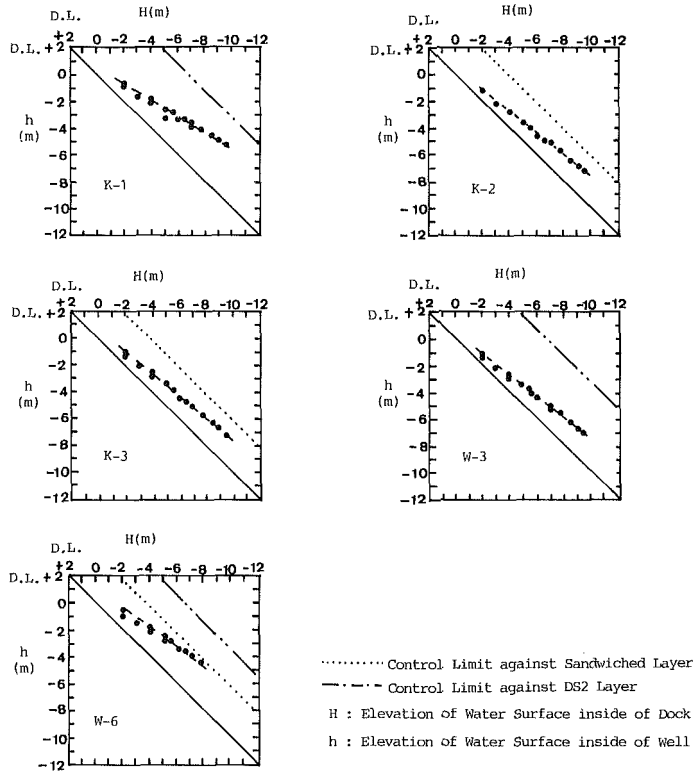

FIG. 5. Control Charts against Underground Water Pressure during Dewatering

water in the dock to a level wherein balance between dead load (i.e., underwater weight of mudstone over the aquifer) and uplift pressure can be maintained. Control limits, the difference in the elevation of the water surface inside of the dock and the wells, are 1.9 m for DS1, 3.9 m for the sandwiched layers, and 6.7 m for DS2. Some of the control charts thus developed are shown in Fig. 5.

These control charts are used to determine the succeeding elevations to which water level inside the dock may be safely lowered. The relation between H (elevation of water surface inside the dock) and h (elevation of water surface inside the wells) does not necessarily lie on one straight line. Hence, to determine H, first, measure the h value at every well, then find the H value as mapped by the control limit lines on the pertinent charts. The largest H value obtained indicates the next elevation to which the water level may be safely lowered. This procedure was repeated until the dock was completely dewatered.

Visual inspection upon dewatering readily confirmed the fact that underground water was indeed seeping through the open joints and cracks in the mudstone layers. In addition, these water paths did not undergo any hydraulic characteristic changes such as loading, thus proving the correctness

of the control charts and showing that the relation between H and h did lie on one straight line throughout the entire process.

Final Confirmation through Test Operation

It is significant to note that this dewatering process took 24 days to complete, while normal operation of the dock will eventually require water to be pumped out within 1–2 hours. The impact of this time difference on quality must be evaluated first by simulation, then by actual on-site tests. It is necessary to check if underground water pressure declines low enough to a safe head within the short time water is pumped out, and whether the water pressure reducing system functions as planned. (This system is composed of crushed gravel and perforated pipes laid under the bottom slab to accumulate and lead water into the pump room. The water is then pumped out so that uplift pressure is not constantly exerted on the bottom slab.)

The effectiveness of the water pressure reducing system is checked at M-1 and M-2 (Fig. 1). The pressure of the confined aquifers is checked at W-6, which is indicated by the control chart (Fig. 5) to be the critical well for determining pressure level decreases. Test operations were carried out at different pumping speeds. Test results using the standard pumping rate during actual operations are shown in Fig. 6. The results confirm the quality of the design and the dock's fitness for use.

Comparison of Estimated and Actual Seepage Volume

An estimated seepage volume was calculated based on the hypothesis that the dock length (180 m) is so long that seepage flow can be idealized by the two-dimensional finite element method. The basic formula (Akai et al. 1977) used for analysis was:

$$\nabla[k(h_p) \cdot \nabla(h_p + h_e)] = [C(h_p) + \alpha \cdot S] \frac{\partial h_p}{\partial t}$$

wherein, k = permeability coefficient; h_p = pressure head; h_e = potential head; $C(h_p)$ = specific water capacity; S = storage coefficient; $\alpha = 0$ = unsaturation zone; and $\alpha = 1$ = saturation zone. Aquifer parameters, analysis conditions, boundary conditions, and initial conditions are introduced into this equation. Permeability coefficient k, having the greatest influence on seepage volume, is established as follows.

The JFT test has shown that the permeability coefficient of DS2 is $k = 1.49–2.10 \times 10^{-3}$ cm/s. On the other hand, the theoretical transmissivity of DS2 may be obtained from the regression formula used in Fig. 4, which was based on Jacob's solution as having the largest correlation coefficient among the four techniques for analysis in Table 2. By substituting $x = 0$ (where vertical leakage can be considered not to occur at all) into the regression formula, theoretical transmissivity $T = k \times t = 1.15 \times 10^{-3}$ m^2/min was obtained. Since the thickness (t) of DS2 is 10–20 cm, $k = 0.96–1.92 \times 10^{-2}$ cm/s. A 10^{-1} order difference between the two k values may be seen, and adopted permeability coefficients have yielded estimates of seepage volume to be 200 m^3/day for the JFT test, and 500 m^3/day based on statistical analysis. The results are summarized in Table 3.

Actual seepage volume measured for the 8-month period immediately after completion showed an average daily volume of 800 m^3. This figure is closer

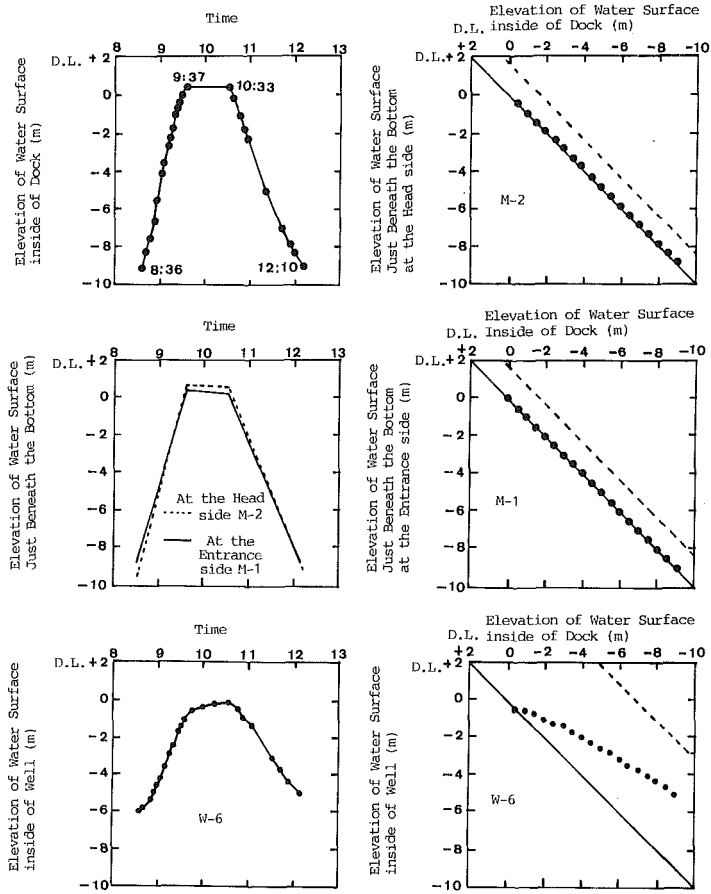

FIG. 6. Final Confirmation through Test Operation

TABLE 3. Adopted Permeability Coefficients for Analysis and Estimated Seepage Volume

Permeability coefficient k (cm/s) (1)	Transmissivity T (m^2/min) (2)	Adopted permeability coefficient k' (cm/s) (3)	Estimated seepage volume (m^3/day) (4)
(*a*) JFT Test Result			
$1.49–2.10 \times 10^{-3}$	$(0.89–2.52 \times 10^{-4})$[a]	1.00×10^{-3}	200
(*b*) Statistical Treatment Result Based on Jacob's Solution			
$(0.96–1.92 \times 10^{-2})$[a]	1.15×10^{-3}	1.00×10^{-2}	500

[a]Results obtained from $T = kt$, where the t = thickness of confined aquifer (10–20 cm) is indicated with parentheses.

to the estimate based on statistical analysis. This is taken to indicate the correctness of the statistical analysis of the pumping test results and the hypothesis of vertical leakage, the validity of the simulation model and analytical method, and that execution has been carried out as planned.

Behavior of Structures

Behavior of Starboard Wall

As has been mentioned, the starboard and head walls are double sheet-pile wall structures, and the portside wall is a gravity-type quay wall made of discarded ship hulls filled with sand. Although much has been published on the subject of double sheet-pile wall structures, very little information is available regarding their deflection characteristics due to alternating loads. It is difficult to quantitatively understand in advance the behavior of double sheet-pile wall structures, specially since the uneven settling of sand particles due to size is inherent to filling work.

In order to insure construction safety during dewatering and to confirm product quality through test runs, the behavior of the structures have been measured with transits and clinometers. The mounting position of the clinometers is shown in Fig. 1.

Deflection of Starboard Wall

Horizontal deflection at the top of the double sheet-pile wall can be calculated using the following Sawaguchi equation (Sawaguchi 1974):

$$Y_t = \frac{mH^5}{60EI}\Phi_5(\lambda H) = \frac{mH^5}{60EI}\left[\frac{5}{(\lambda H)^2} + \frac{30}{(\lambda H)^4} - \frac{15(2+\lambda^2 H^2)}{(\lambda H)^6}\tanh(\lambda H)\right]$$

wherein Y_t = deflection at the top of the wall; m = incremental rate of hydrostatically distributed pressure in relation to depth; H = effective height of the structure; EI = flexural rigidity of sheet piles per unit width; and $\lambda = \sqrt{[BG/(2EI)]}$, wherein B = width of the structure; and G = modulus of rigidity of the filling, such that $G = E_s/3$ (where E_s = Young's modulus of the filling).

Young's modulus of the filling is obtained using a presiometer located at two points in the starboard wall. Test results, summarized in Table 4, show that Young's modulus varies greatly for each of the tested depths. The relation between Young's modulus and depth is shown in Fig. 7. By evaluating the Sawaguchi equation using $E_s = 34.6 \fallingdotseq 30$ kg/cm^2 (Young's modulus at the midpoint depth of the starboard wall), calculations were made for every water surface level inside the dock. Calculation results are shown in Fig. 8.

TABLE 4. Young's Modulus of Filling by Horizontal Loading Test (kg/cm^2)

Boring location (1)	Measured Depth		
	3.0 m (2)	6.0 m (3)	9.0 m (4)
No. 1	7.0	36.5	33.9
No. 2	11.7	6.9	57.9

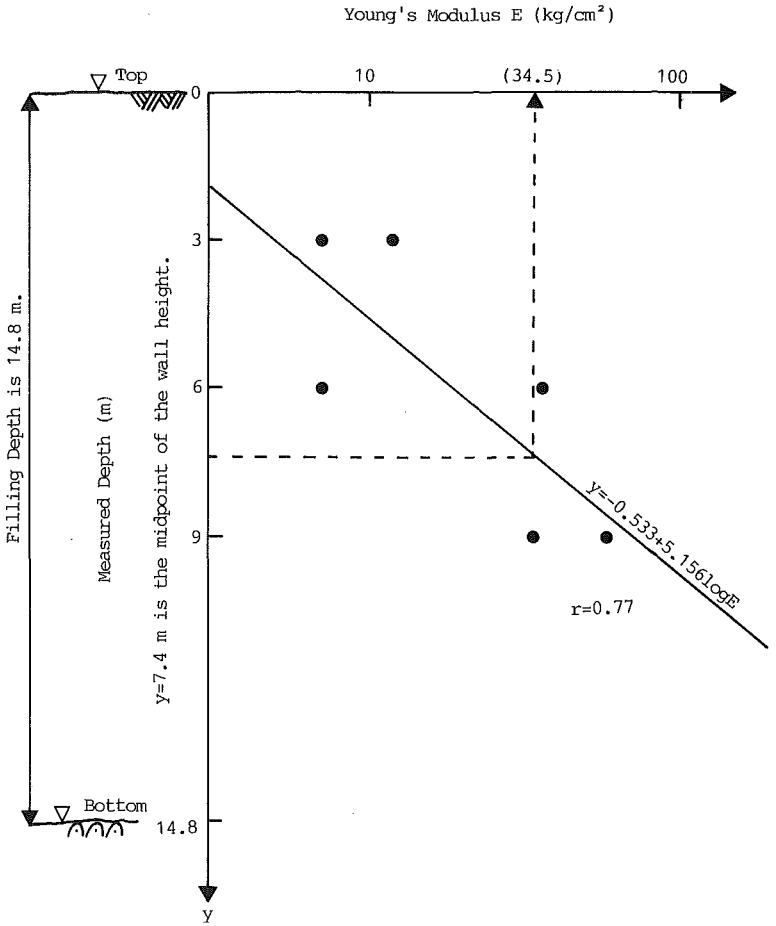

FIG. 7. Relation between Young's Modulus and Filling Depth

Comparison of Actual and Calculated Deflection

The large difference at an early stage between the measured values of deflection at clinometer No. 2 and clinometer No. 3 eventually becomes smaller in time (Fig. 8). This difference is caused by the location of the clinometers. Clinometer No. 2 is located at the center of the starboard wall while clinometer No. 3 is nearer the head wall. The head wall thus functions as a support, and the partition pile walls at the junction of the starboard and head help reduce deflection (Fig. 1).

A comparison of the measured and calculated deflection shows that actual deflection has not occurred simultaneously with the change in load (decline in the water level), but has lagged behind in time. The calculated final deflection approximates very closely the measured values. This may be attributed to the construction of the starboard wall on the ground layer, resulting in a structure closely resembling Sawaguchi's original model. It likewise indicates that the value used as modulus in the calculations was applicable.

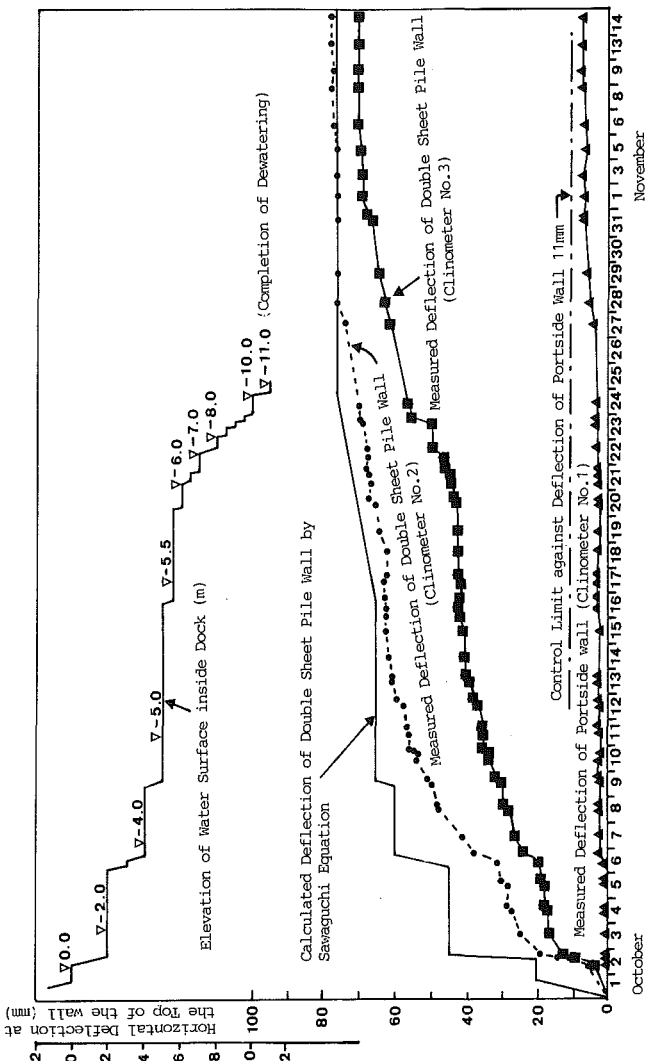

FIG. 8. Deflection Characteristics during Dewatering

J. Constr. Eng. Manage., 1990, 116(2): 201-220

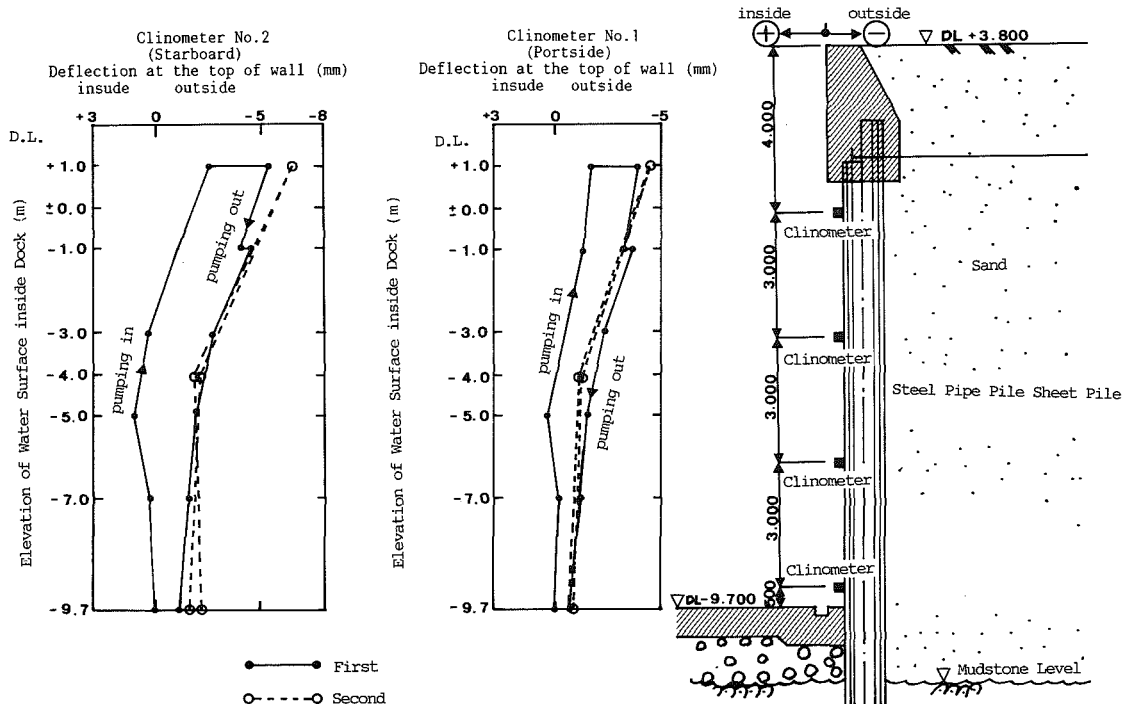

* Locations of the clinometer in the plane are illustrated in Fig.1.
** Clinometers are mounted at the same level as the portside.

FIG. 9. Deflection Characteristics due to Periodic Loading

Deflection due to Periodic Loading

The deflection characteristics of the starboard wall as it is dewatered for a second time is shown in Fig. 9. The curve formed by the second loading approximates the curve obtained when the dock was refilled after initial dewatering. The third and fourth dewatering tests produced the same curve as the second.

The similarity of the curves is thought to indicate that the ratio of effective height of the structure (H = 14.8 m) to the maximum lateral deflection at the top of the wall (Y_t = 6.5 mm) is so small (0.04%) that the shearing strain in the filling remains within the elasticity limit.

Close inspection of the concrete coping on the sheet pile did not reveal any cracks or defects.

Behavior of Portside Wall

The quay wall was constructed as a landing pier 25 years ago using discarded ship hulls anchored on a riprap mound. Its converted use as the portside wall of the dock subjects it to considerable pressure, especially during dewatering. Structural stability against overturning and bearing capacity has been certified by the construction records of previous projects. Lateral sliding of the wall has been prevented during construction by underwater concrete struts, and after completion by the bottom slab.

However, the difference in level between the left and right rail of the jib crane mounted on the wall, brought about by rotation, must be within 11 mm. Since it was not possible to test the reaction of the riprap mound, corrective countermeasures, such as the insertion of concrete sleepers under the rails, were considered should rotation exceed allowable limits.

The deflection of the portside wall was measured during dewatering and the test operation. Results are shown in Figs. 8 and 9. The rail level difference (D_v) was obtained by using the equation D_v = rail-to-rail distance/height of ship hull $\times$ D_H, where D_H is the deflection at the top of the wall. This was also confirmed by a leveling survey. During dewatering, maximum D_H was 7.5 mm, resulting in D_v of 5.5 mm. During the test operation, maximum D_H was 4.0 mm, and D_v was 3.0 mm.

Conclusion

While significant differences between construction and manufacturing hinder the development of integrated technology and quality control, it should be emphasized that construction management must be supported by scientific theory (Kumamoto and Hoshiya 1985). The more complex and unique projects are, the more necessary innovative technology and quality control become. Management methods that have proved highly successful in the manufacturing industry are not always applicable in detail to civil engineering management because the conditions are very different. First, construction involves uncertainty. Second, the projects are unique. Specific conditions vary from site to site, and projects are rarely repeated exactly. Third, construction projects do not allow for test products. Experiment samples may not be made as the projects are the final products in themselves. Fourth, imput from the latest finished phases of a construction project must often be immediately synthesized to determine the appropriate methods for the next phase. The degree of project efficiency and success, therefore, depends pri-

marily on senior professional personnel who have good engineering and managerial ability backed not only by empirical but also by scientific principles.

APPENDIX. REFERENCES

Akai, K., Ohonishi, Y., and Nishigaki, M. (1977). "Finite element analysis of saturated-unsaturated seepage in soil." *Proc.*, Japan Society of Civil Engineers, 264, 87–96 (in Japanese).

Hantush, M. S. (1960). "Flow to an eccentric well in a leaky circular aquifer." *J. Geophysical Reference,* 65(10), 3425–3431.

Kumamoto, T., and Hoshiya, M. (1985). "Introduction of reliability analysis into shield construction management." *Proc. 4th Int. Conf. on Struct. Safety and Reliability,* International Association for Structural Safety and Reliability and ASCE.

Kumamoto, T., and Hoshiya, M. (1987). "Probabilistic evaluation of alternatives for structures under construction." *Proc.*, Japan Society of Civil Engineers, 385(6–7), 88–97 (in Japanese).

Peck, R. B. (1969). "Advantages and limitations of the observational method in applied soil mechanics." *Geotechnique,* 19(2), 171–187.

Sawaguchi, M. (1974). "Lateral behavior of a double sheet pile structure." *Proc.*, Japanese Society of Soil Mechanics and Foundation Engineering, 14(1), 45–59.

Thesis, C. V. (1935). "The relation between the lowering of the piezometic surface and the rate and duration of discharge of a well using ground water storage." *Trans.*, American Geophysics Union, 16, 519–524.